Comparison of PMSMs Motor Current Signature Analysis and Motor Torque Analysis Under Transient Conditions

Comparison of PMSMs Motor Current Signature Analysis and Motor Torque Analysis Under Transient Conditions.

1st Andrea Bonci
Dept. of Information Engineering
Polytechnic University of Marche
Ancona, Italy
a.bonci@univpm.it

2nd Marina Indri
Dept. of Electronics and Telecommunication.
Politecnico di Torino
Torino, Italy
marina.indri@polito.it

3rd Renat Kermenov*
Dept. of Information Engineering
Polytechnic University of Marche
Ancona, Italy
r.kermenov@pm.univpm.it

4th Sauro Longhi
Dept. of Information Engineering
Polytechnic University of Marche
Ancona, Italy
sauro.longhi@univpm.it

5th Giacomo Nabissi*
Dept. of Information Engineering
Polytechnic University of Marche
Ancona, Italy
g.nabissi@univpm.it

***Abstract*—PMSMs are widely used in applications on electric vehicles, robotics and mechatronic systems of industrial machinery. Thus it becomes increasingly interesting to prevent their fault or malfunctioning with Predictive Maintenance (PdM). However, reaching this outcome could be difficult, especially if the stationary condition is not achieved and without additional sensors. This paper examines the use of a load torque observer based on Extended Kalman Filter for the diagnosis of electric drives working under non-stationary conditions. The proposed Motor Torque Analysis (MTA) is compared with the Motor Current Signature Analysis by evaluating their diagnostic capabilities under the assumed conditions. Finally, the results of bearing failure detection under non-stationary conditions are presented, highlighting the superior diagnostic capabilities of the MTA under such conditions.**

***Index Terms*—PMSM, non-stationary detection,MCSA-Motor Current Signature Analysis, MTA-Motor Torque Analysis, EKF-Extended Kalman Filter.**

I. Introduction

Permanent magnet synchronous motors (PMSMs) are electric drives widely used in a wide range of industrial and engineering fields due to their reliability, ruggedness and simple construction. These motors are used in applications on electric vehicles, in robotics and mechatronic systems of industrial machinery, which will be an integral part of the upcoming cyber-physical production systems [1]. Due to their spread in the above-mentioned applications, and their key role [2] in guaranteeing performance and safety conditions of systems [3], [4], it becomes increasingly interesting to prevent their fault or malfunctioning with predictive maintenance (PdM). Among the established techniques used for PdM, the Motor Current Signature Analysis (MCSA) is one the most used for induction motors (IMs) [5], but it is also applied to PMSMs under certain working conditions [6]. Other established condition monitoring techniques often include vibrations, especially for mechanical fault diagnosis in steady-state conditions. However, it is more invasive since sensors must be installed on the drive, while MCSA requires only current sensors. It is simply based on electric measurements of the motor current that are analysed using Fourier analysis. Indeed, under the assumption of constant or quasi-constant speed, motor faulty conditions can be detected in the signal power spectrum. However, when the constant speed may not be guaranteed, faulty behaviour can be masked and damped by the supply harmonics. Indeed, in many systems actuated by PMSMs, constant speed assumption is unrealistic and faulty harmonics in the power spectrum are hardly identifiable. This is due to the rapid change of the electric signal, which crosses different frequencies over time. In such cases, diagnosis with MCSA could results unreliable if merely applied to transient conditions, as highlighted both in robotic applications [7] and in industrial machinery [8]. Motors' diagnosis in non-stationary conditions can be relevant for different purposes, such as those involving control, safety, or evaluation of health conditions. Just think to the forthcoming electric vehicles equipped with all-wheel drive, whether they are four or two-wheel drive [9], [10], where the motors rapidly changing speed. Furthermore, all applications with torque control for

*R.Kermenov and G. Nabissi contributed equally to the idea and results obtained in this work as first authors.

This work was supported by the EU H2020 ENCORE Project under Agreement 820434, by the REACT Project from the Italian Ministry of University and Research (MIUR)-in National Operative Plan (PON) for Research and Innovation 20142020, under Project ARS01 01031, and by the HD3Flab Project "Human Digital Flexible Factory of the Future Laboratory" EU ERDF (European Regional Development Fund), Regional Operative Plan (POR) MARCHE Region FESR (Fondo Europeo di Sviluppo Regionale) 2014/2020, AXIS 1, Specific Objective 2, ACTION 2.1

fast precise tasks, for instance, robotic collaborative tasks or high-performance mechatronic systems are of interest. In high performances electrical drives, observers are often used as established techniques to replace sensors; very often load torque observers are used for control purposes [11], [12]. This because torque sensors are often bulky and expensive. Thus, they cannot be a good choice for most applications, while torque estimation allows having a cost-less, reliable, and more compact drive system. Only Stopa et al. [13] propose for the first time a load torque analysis investigating the mathematical relationships and the frequency response using the linear Luenberger observer for IMs. However, their approach is applicable only to motor running at a constant speed and requires additional voltage sensors for magnetic flux and electromagnetic torque estimation. On the other hand, condition monitoring and diagnosis of electrical drives using observer-based methods in non-stationary conditions are not well established. The present paper intends to investigate the usefulness of a load torque observer for diagnosis on electric drives working in non-stationary conditions. Results are evaluated comparing the MTA with the most widely used technique that uses the same signals for diagnosis (MCSA). Both techniques do not require the installation of additional sensors except those already present in the drive. The paper is organised as follows: section II introduces the PMSM model and the torque estimation problem, section III shows the results, while section IV concludes the paper.

II. PMSM MODELING AND LOAD TORQUE ESTIMATION

A. Mathematical model of the PMSM

Referring to the well known model of a PMSM in Park's domain [14], the relation between the three-phase currents I_a, I_b, I_c and the direct, quadrature, and zero current components I_d, I_q and I_0 in a rotating reference dq-frame is

$$\begin{bmatrix} I_d \\ I_q \\ I_0 \end{bmatrix} = \begin{bmatrix} \cos(\theta_e) & \cos(\theta_e - \frac{2\pi}{3}) & \cos(\theta_e + \frac{2\pi}{3}) \\ -\sin(\theta_e) & -\sin(\theta_e - \frac{2\pi}{3}) & -\sin(\theta_e + \frac{2\pi}{3}) \\ 1/2 & 1/2 & 1/2 \end{bmatrix} \begin{bmatrix} I_a \\ I_b \\ I_c \end{bmatrix} \tag{1}$$

where $\theta_e = P \cdot \theta_m$ is the electrical position of the dq-frame in radiants, θ_m is the angular position, and P is the pole number. According to this model, two electric equations can be derived:

$$V_d = R_s I_d + L_d \frac{dI_d}{dt} - P\omega_r L_q I_q, \tag{2}$$

$$V_q = R_s I_q + L_q \frac{dI_q}{dt} + P\omega_r (I_d L_d + \phi_{pm}), \tag{3}$$

where V_d and V_q are the voltages in the Park domain, R_s, L_d and L_q are the electric parameters of the equivalent circuit of the stator, ω_r is the angular velocity of the rotor and ϕ_{pm} is the permanent magnet flux linkage. The electromagnetic torque can be estimated as:

$$T_e = \frac{3}{2} P\, I_q(\phi_{pm} + I_q(Ld - Lq)). \tag{4}$$

The assumption of non salient poles implies that $L_d = L_q = \frac{L_s}{2}$, and the equation (4) is simplified as follows:

$$T_e = \frac{3}{2} P I_q \phi_{pm}. \tag{5}$$

In addition to the electric equations, we define the well known mechanic equations of the rotor:

$$\frac{d\omega_r}{dt} = \frac{1}{J}(T_e - T_l), \tag{6}$$

$$\frac{d\theta_e}{dt} = P\omega_r. \tag{7}$$

The load toque T_l is assumed to vary slowly w.r.t. the dynamics of the electric equations which changes rapidly, and w.r.t. the sample time ($t_s \simeq 10^{-5} sec$). Thus, we can assume it to be constant during a sampling period without lost of information:

$$\frac{dT_l}{dt} \simeq 0. \tag{8}$$

The state vector x, the input vector u and the output vector y of the state space representation are chosen as $x = [I_d,\, I_q,\, \omega_r,\, \theta_e,\, T_l]^T$, $u = [V_d,\, V_q]^T$ and $y = [I_d,\, I_q,\, \omega_r,\, \theta_e]^T$. According to forward Euler approximation, we can obtain the discrete time state space system representation as follows:

$$\begin{aligned} x_{k+1} &= f(x_k, u_k) + w_k = A(x_k)x_k + Bu_k + w_k \\ y_k &= h(x_k) + v_k = Cx_k + v_k \end{aligned} \tag{9}$$

where:

$$\begin{aligned} A(x_k) &= \begin{bmatrix} 1 - T_s\frac{R_d}{L_q} & T_s\frac{L_d}{L_q} & 0 & 0 & 0 \\ -\omega_r T_s \frac{L_d}{L_q} & 1 - T_s\frac{R_s}{Lq} & -T_s p \phi_{pm} & 0 & 0 \\ 0 & \frac{3}{2}\frac{p}{J}\phi_{pm} & 1 & 0 & -\frac{T_s}{J} \\ 0 & 0 & T_s p & 1 & 0 \\ 0 & 0 & 0 & 0 & 1 \end{bmatrix} \\ B &= \begin{bmatrix} \frac{T_s}{L_d} & 0 \\ 0 & \frac{T_s}{L_q} \\ 0 & 0 \\ 0 & 0 \\ 0 & 0 \end{bmatrix} \quad C = \begin{bmatrix} 1 & 0 & 0 & 0 & 0 \\ 0 & 1 & 0 & 0 & 0 \\ 0 & 0 & 1 & 0 & 0 \\ 0 & 0 & 0 & 1 & 0 \end{bmatrix} \end{aligned} \tag{10}$$

with w_k and v_k, respectively, the process and observation noises which are assumed to be zero mean Gaussian variables with covariances:

$$Q = \begin{bmatrix} 0.1 & 0 & 0 & 0 & 0 \\ 0 & 0.1 & 0 & 0 & 0 \\ 0 & 0 & 0.1 & 0 & 0 \\ 0 & 0 & 0 & 0.1 & 0 \\ 0 & 0 & 0 & 0 & 1 \end{bmatrix}, R = \begin{bmatrix} 0.25 & 0 & 0 & 0 \\ 0 & 0.25 & 0 & 0 \\ 0 & 0 & 0.5 & 0 \\ 0 & 0 & 0 & 0.5 \end{bmatrix}. \tag{11}$$

Q and R will play the role of design matrices of the Extended Kalman Filter and have been chosen using a trial-and-error approach; further details regarding the choice are given in Section II-B1.

B. EKF load torque estimation

The EKF is the tool chosen to estimate the load torque T_l, i.e., one of the state vector variables [11]. Table I summarizes the steps of the EKF algorithm. In our notation F_k and H_k are the state transition and observation matrices defined respectively as:

$$F_k = \frac{\partial f}{\partial x}|_{x_{k-1|k-1}, u_k},\; H_k = \frac{\partial h}{\partial x}|_{x_{k-1|k-1}}. \tag{12}$$

Matrices $P_{k|k-1}$ and $P_{k|k}$ are the predicted and innovated state covariances respectively. The Initialization values for the EKF algorithm (Tab. I) are as follow:

$$\begin{aligned} P_{0|0} &= diag\begin{bmatrix} 0.1 & 0.1 & 5 & 1 & 10 \end{bmatrix} \\ x_{0|0} &= \begin{bmatrix} 0 & 0 & 0 & 0 & 0 \end{bmatrix}^T. \end{aligned} \tag{13}$$

TABLE I
THE EKF ALGORITHM

Prediction step
$x_{k\|k-1} = A(x_k)x_{k-1} + Bu_k$
$P_{k\|k-1} = F_k P_{k-1\|k-1} F_k^T + Q$
Innovation step
$K_k = P_{k\|k-1} H_k^T (H P_{k\|k-1} H^T + R)$
$x_{k\|k} = x_{k\|k-1} + K_k(y_k - H x_{k\|k-1})$
$P_{k\|k} = P_{k\|k-1} - K_k H P_{k\|k-1}$

1) Design and tuning of Q, R, $P_{0|0}$: The critical point for the EKF design is the choice of the covariances matrices which affect the performance and the convergence of the observer as well [12]. Varying $P_{0|0}$ yields to a different amplitude of the transient, but does not affect transient duration and steady-state conditions. Q gives a statistical description of the reliability of the model and of the parameters uncertainty. R is related to measurements noise. Higher the values, lower the confidence in the measurements.

C. Bearing fault modelling

The model of a bearing fault proposed in [15] states that this fault can be observed by the dynamic rotor equation:

$$\frac{d\omega}{dt} = \frac{1}{J}(T_e - \beta(\theta_r)\omega_r - T_l), \tag{14}$$

where:

$$\beta(\theta_r) = \beta \triangle_\beta \tag{15}$$

describes an inner bearing section behavior that varies linearly with respect to the angular position. With respect to (6), equation (14) contains an additional term that the EKF observer confuses in the T_l estimation. Then, from now on, we will distinguish the real torque T_l by the torque T_{lo} estimated with the Extended Kalman Filter. This last contains two different quantities when a mechanical fault arises (e.g., bearing fault). One is related to the torque load and the other one depends on the fault contribution, as follows:

$$T_{lo} = T_l + \beta(\theta_r)\omega_r. \tag{16}$$

Consequently, in order to detect this fault, we can analyse the signal T_{lo} that comes out from our observer and from this information pull out the faulty therm. Trivially in this paper, the magnitude of the signal is evaluated and a threshold is selected to detect the defecting frequencies. In the following section we investigate the proposed approach.

III. RESULTS

In this Section, experimental and simulation results are compared first to validate the dq-model of the PMSM, derived in Section II. Equation (10) represents the state-space model of the industrial PMSM (Fig. 1) whose parameters are listed in Table II. Then, the EKF is used in simulation to estimate the torque load T_l (eq.(6)) in both cases of healthy conditions and bearing fault (eq. (15)).

A. PMSM model validation

To validate the PMSM model, the currents of the two phases (I_a, I_b) and the rotor position are acquired from the real asset (Fig. 1). Having the measurements of the two phases currents the third one can be simply derived from $I_a + I_b + I_c = 0$. The rotor position measurements (θ_r) is used to calculate the d and q current components of the Park transform using equation (1). Through equations (2), (3), (6) (7) and the I_d, I_q signals obtained from the real PMSM, it is possible to compare dynamic behaviours of the real asset with its model, as shown in Figure 2. Then, the Root Mean Square Error (RMSE) between the two w_r signals is calculated to validate results as

$$RMSE = \sqrt{\frac{1}{N}\sum_{k=1}^{N}(y_k - \hat{y_k})^2}, \tag{17}$$

where $y_k, \hat{y_k}$ are the real and simulated ω_r and N is the length of the signals. As shown in Figure 2, the dynamic behaviour of the model is very consistent. The w_r signal obtained from simulations is almost perfectly overlapped to the real one, the RMSE value is $\simeq 0.70$. The diagnosis with MTA is compared with MCSA technique using the PMSM model in a double loop control scheme commonly used in electric motors [16]. The entire architecture is presented in Figure 3, here is possible to notice the controllers and EKF observer interaction, the measured signals and the estimated ones. The V_d and V_q voltage references to the Inverter source are converted into the effective open and closure of the IGBTs (three-phase AC) using the Space Vector Pulse With Modulation (SV-PWM) technique [16].

B. Bearing fault analysis

The bearing fault can be modelled using a friction function $\beta(\theta_r)$ (eq. (15)) as presented above. As already showed in different work, in case of steady-state application (constant reference speed) bearing faulty frequencies (f_{bf}) can be detected in the one-phase currents harmonics using MCSA [17], [18]. These frequencies depend on the rotor position θ_r and then in the motor speed ω_r:

$$f_{bf} = \pm k\, f_r. \tag{18}$$

where k is any integer and f_r is the rotational frequency of the rotor. However, in general it may be difficult to detect mechanical faults in the current spectrum, especially when the constant speed assumption can not be fulfilled. Usually, advanced signal processing tools have to be used to extract faulty features from these signals. Indeed, in case of mechanical faults under non-stationary conditions the faulty frequencies in the current spectrum can be masked or damped. The motor supply frequency and its harmonics mask and overhang mechanical defecting frequencies that show a lower contribute. This last assertion has been already proven in two other previous works [7], [8], but more details will be clearer during the results discussion. Thus, since mechanical faulty frequencies observed in the current spectrum are caused by

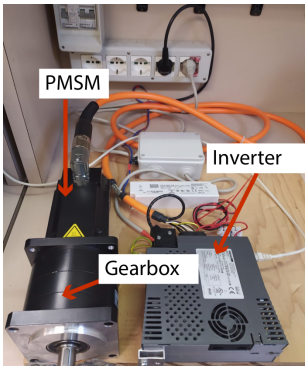

Fig. 1. Laboratory test bench developed by the authors using an industrial electric motor. (PMSM)

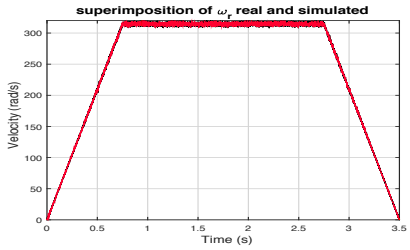

Fig. 2. Superimposition of the w_r signals, in red the simulated while in black the real feedback of the PMSM.

anomalous oscillations produced by a mechanical defect in the rotor shaft, in the transmission system or the load, we propose to use an EKF load torque observer to detect and diagnose this behaviour. The estimated signal (T_{lo}) is analysed to extract faulty characteristic. We remark that the torque load signal does not contain electric frequencies related to the motor supply, leading to analyse a signal without additional information not useful for diagnosis.

C. Results discussion

The filtered and estimated state vector $\hat{x} = [I_d,\, I_q,\, \omega_r,\, \theta_e,\, T_{lo}]$ obtained with the EKF is presented in Figure 4. The reference speed profile used (Fig. 3) is a trapezoidal speed-time curve. Attached to the motor shaft is modelled a load torque of $0.5\,Nm$ with relative coefficient friction $\boldsymbol{\beta}$ listed in Table II. Two different simulations are conducted running the PMSM in case of healthy conditions and in case of bearing fault. During the simulations are acquired the one-phase current I_a and the T_{lo} signal with a sampling frequency of 2 kHz. The first signal is used to perform MCSA, while the signal obtained with the observer is used for MTA.

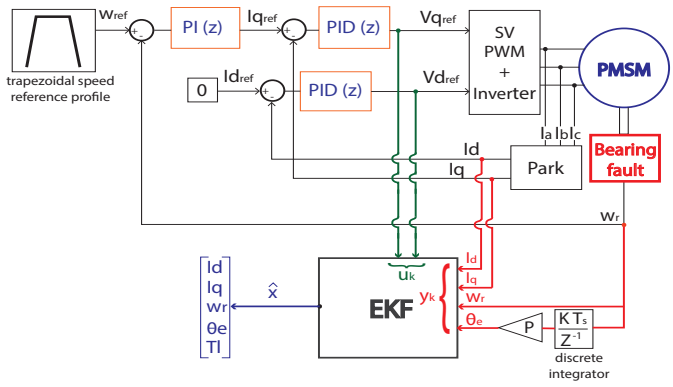

Fig. 3. Double velocity loop control scheme used in simulation. The blue PMSM represents the model of the electric drive while the red cube represents the bearing fault model. The EKF is drawn in the bottom part of the image with input u_k, measurement y_k and prediction $\hat{x}$.

1) The priory knowledge: Considering the reference trapezoidal speed-time curve that goes from 0 to 288 $[rad/s]$ (Fig. 4), having a priory knowledge on the fault behaviour we already know which frequencies should be monitored according to equation (18). The trapezoidal speed signal reaches for a short period ($\simeq 1\,sec$) the constant velocity shape ($w_r = 288\,[rad/s]$), while for the remaining time a constant acceleration profile is applied with varying speed. In the constant speed period, the rotational frequency is equal to $f_r = 45.83[Hz]$. Thus, according to (18) in the current signal (I_a) and in the estimated torque load signal (T_{lo}) we look for harmonics related to f_r which indicate that a bearing is broken.

Figure 5 shows the one-phase measured current and its FFT when the PMSM is running in healthy conditions. While Figure 6 shows the same one-phase current acquisition and relative FFT when the bearing fault arises. As it is possible to notice, the FFT of the current signal presents all the frequencies crossed over time with a bigger peak related to the inverter supply on $f_e = 229.15\,Hz$ (upper image of Fig. 5). This peak is related to the short period of constant speed assumption ($f_r = 45.83,\, Hz$) considering that the electric supply frequency $f_e = P\,f_r$ where P is the poles pairs. Since we are working with a synchronous motor, in which the rotational frequency (f_r) is synchronous with the supply frequency (f_e), we have that f_e starts from 0 Hz, goes to 229.15 Hz and comes back to 0 Hz in 3.5 sec to follow the trapezoidal speed reference profile. This causes the spread of the frequencies in all the spectrum of the measured one-phase electric signal because of non-stationary conditions. The analysis of this signal and the detection of the frequency peak related to the bearing fault is hard without using advanced processing techniques. Indeed, most of the defecting frequencies are damped by electrical frequencies related to the supply, as it is clearly visible in the upper image of Figure 6 by evaluating the signal frequency content. Regarding the proposed MTA, Figure 7 shows the T_{lo} estimation in case of healthy conditions and its FFT. While in Figure 8 is shown the T_{lo} estimation in case of bearing fault with relative FFT. As it can be seen, the fault signature is clearly visible in the T_{lo} spectrum and can be identified by considering the frequency difference between 7 and 8. Referring to the measured one-phase current I_a, the T_{lo} signal may contain frequencies only when mechanical malfunctions arise. Indeed, in case of healthy conditions T_{lo} does not contain any frequency content. Comparing diagnosis results of MTA and MCSA,

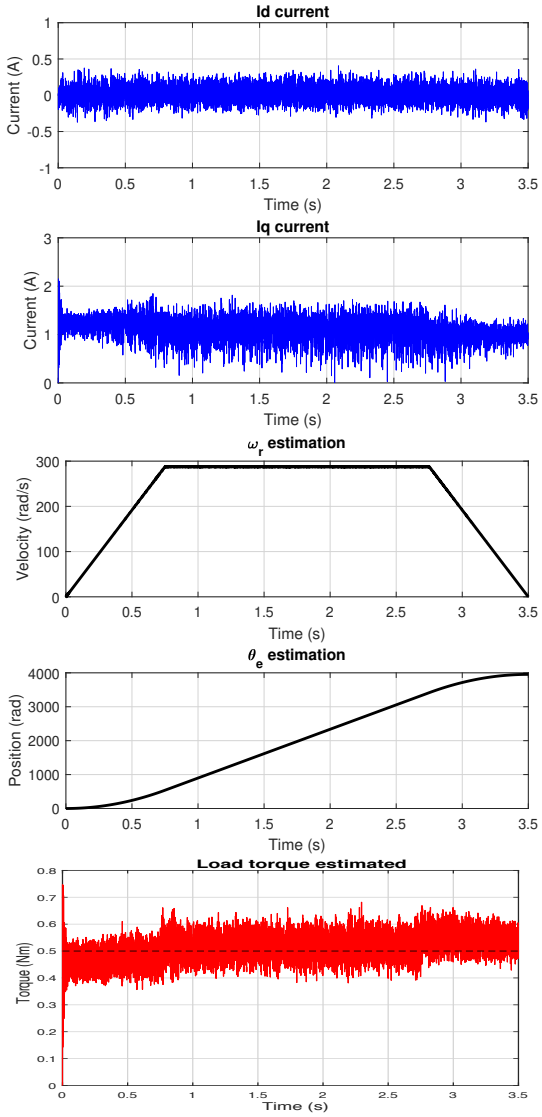

Fig. 4. I_d, I_q, ω_r, θ_e, T_{lo} estimation in case of PMSM healthy conditions. Starting from the bottom in red the T_{lo} signal acquired during trapezoidal speed-time curve ω_r. In black the electric position θ_e of the dq-frame and ω_r estimation, while in blue the dq currents.

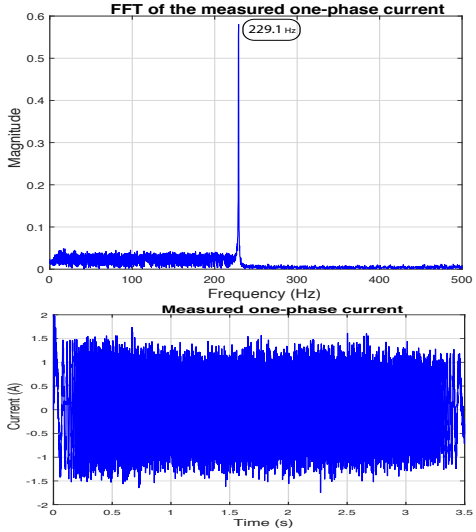

Fig. 5. In the bottom image is shown the I_a current in case of healthy conditions, while the upper image shows the FFT of the I_a signal.

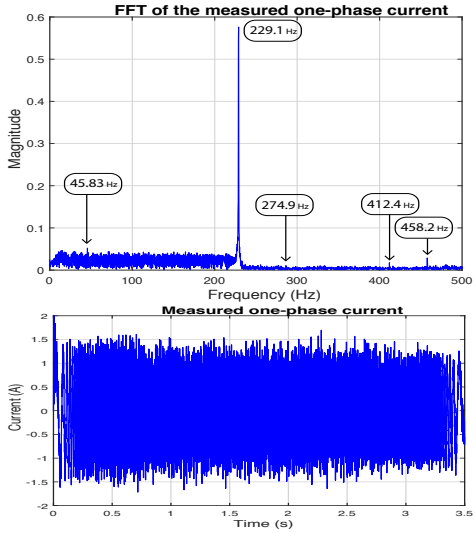

Fig. 6. In the bottom image is shown the I_a current in case of bearing fault, while the upper image shows the FFT of the I_a signal.

shown in Figure 6 and Figure 8 respectively, can be evidenced the superior capability of MTA of detecting failures in non-stationary conditions. Using MTA, even under non-stationary conditions it is straightforward to detect defecting frequencies. Regarding the shape of the T_{lo} signal, it can be noticed that it strictly depends on the dynamics behaviour of the PMSM. This depends on how much accurately is modelled the load torque equation. The robustness of the torque estimation by EKF has been already analyzed in [12] and [19]. Since we assume that the variation of the load torque ($\dot{T}_l$) is zero in a small period, only when the constant speed phase is reached the T_l value is well estimated, as clearly explained in [19]. During transient, indeed, it may be present an amplitude difference depending on the parameters uncertainty (e.g., inertia J, viscous damping β, etc). However, for diagnosis purposes, this does not affect the reliability of the proposed method. Indeed, it is really interesting to notice that the faulty frequencies belonging to the bearing can be easily detected once performed the Fourier analysis on the estimated T_{lo}.

IV. Conclusion and Future Trends

This paper proposes the MTA based on Extended Kalman Filter for diagnosis of electric drives under non-stationary conditions. The observer allows to use the same inputs of MCSA without oversensoring the system. Thus, the results are compared with the well-known MCSA diagnosis technique and superior diagnostic capabilities are shown under the assumed conditions especially for mechanical defects affecting the load torque. In future works, the MTA will be tested introducing failures in the real asset. Furthermore, will be

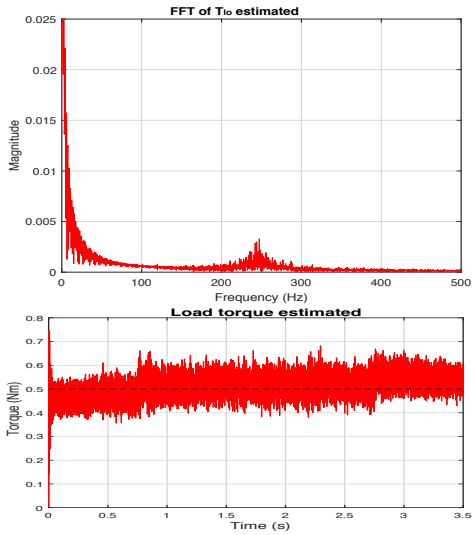

Fig. 7. In the bottom image is shown the T_{lo} obtained with EKF observer in case of healthy conditions with a $T_l = 0.5\,[Nm]$ (dashed black line) while the upper image shows the FFT of the T_{lo} signal.

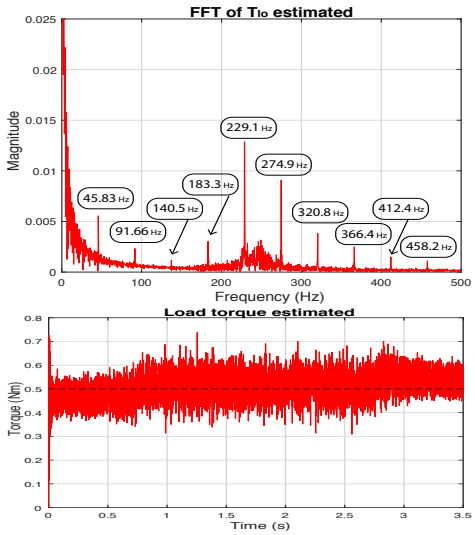

Fig. 8. In the bottom image is shown the T_{lo} obtained with EKF observer in case of bearing fault with a $T_l = 0.5\,[Nm]$ (dashed black line) while the upper image shows the FFT of the T_{lo} signal.

discussed the possibility of using the proposed technique to develop a reliable PdM supervision system.

TABLE II
PMSM PARAMETERS

Resistance (ph-ph)	$\boldsymbol{Rs}$	1.648 $[\boldsymbol{Ohm}]$
Inductance (ph-ph)	$\boldsymbol{Ls}$	0.006011 $[\boldsymbol{H}]$
Flux linkage established by magnets	$\boldsymbol{\phi_{pm}}$	0.0596421 $[\boldsymbol{V.s}]$
Pole pairs	$\boldsymbol{P}$	5
Inertia	$\boldsymbol{J}$	0.0001453 $[\boldsymbol{Kg.m^2}]$
Friction factor	$\boldsymbol{\beta}$	$9.0e-05$ $[\boldsymbol{N.m.s}]$
Bearing friction	$\boldsymbol{\Delta\beta}$	$1e-06$ $[\boldsymbol{N.m.s}]$

REFERENCES

[1] Andrea Bonci, Massimiliano Pirani, and Sauro Longhi. An embedded database technology perspective in cyber-physical production systems. *Procedia Manufacturing*, 11:830–837, 2017. 27th International Conference on Flexible Automation and Intelligent Manufacturing, FAIM2017, 27-30 June 2017, Modena, Italy.

[2] Maria Drakaki, Yannis L. Karnavas, Panagiotis Tzionas, and Ioannis D. Chasiotis. Recent developments towards industry 4.0 oriented predictive maintenance in induction motors. *Procedia Computer Science*, 180:943–949, 2021. Proceedings of the 2nd International Conference on Industry 4.0 and Smart Manufacturing (ISM 2020).

[3] Andrea Bonci, Riccardo De Amicis, Sauro Longhi, Emanuele Lorenzoni, and Giuseppe A. Scala. A motorcycle enhanced model for active safety devices in intelligent transport systems. In *2016 12th IEEE/ASME International Conference on Mechatronic and Embedded Systems and Applications (MESA)*, pages 1–6, 2016.

[4] Andrea Bonci, Pangcheng David Cen Cheng, Marina Indri, Giacomo Nabissi, and Fiorella Sibona. Human-robot perception in industrial environments: A survey. *Sensors*, 21(5), 2021.

[5] Manjeevan Seera, Chee Peng Lim, Saeid Nahavandi, and Chu Kiong Loo. Condition monitoring of induction motors: A review and an application of an ensemble of hybrid intelligent models. *Expert Systems with Applications*, 41(10):4891–4903, 2014.

[6] S. Nandi and H.A. Toliyat. Condition monitoring and fault diagnosis of electrical machines-a review. In *Conference Record of the 1999 IEEE Industry Applications Conference. Thirty-Forth IAS Annual Meeting (Cat. No.99CH36370)*, volume 1, pages 197–204 vol.1, 1999.

[7] Andrea Bonci, Sauro Longhi, Giacomo Nabissi, and Federica Verdini. Predictive maintenance system using motor current signal analysis for industrial robot. pages 1453–1456, 2019.

[8] Andrea Bonci, Sauro Longhi, and Giacomo Nabissi. Fault diagnosis in a belt-drive system under non-stationary conditions. an industrial case study (in press). *2021 5th IEEE Workshop on Electrical Machine Design, Control and Diagnosis (WEMDCD)*, 2021.

[9] Valentin Ivanov, Dzmitry Savitski, and Barys Shyrokau. A survey of traction control and antilock braking systems of full electric vehicles with individually controlled electric motors. *IEEE Transactions on Vehicular Technology*, 64(9):3878–3896, 2015.

[10] Andrea Bonci, Sauro Longhi, and Giuseppe Antonio Scala. Towards an all-wheel drive motorcycle: Dynamic modeling and simulation. *IEEE Access*, 8:112867–112882, 2020.

[11] D. Janiszewski. Extended kalman filter based speed sensorless pmsm control with load reconstruction. In *IECON 2006 - 32nd Annual Conference on IEEE Industrial Electronics*, pages 1465–1468, 2006.

[12] Silverio Bolognani, Luca Tubiana, and Mauro Zigliotto. Extended kalman filter tuning in sensorless pmsm drives. *IEEE Transactions on Industry Applications*, 39(6):1741–1747, 2003.

[13] M. M. Stopa and B. d. J. Cardoso Filho. Load torque signature analysis: An alternative to mcsa to detect faults in motor driven loads. In *IEEE Energy Conversion Congress and Exposition*, pages 4029–4036, 2012.

[14] D. Mondal A. Chakrabarti A. Sengupta. *Power System Small Signal Stability Analysis and Control*. Academic Press, London, 2020.

[15] F. Javier V. Piña, N. Visairo, and R. A. Salas. Mathematical model for electric and mechanical faults in an ac machin. *IFAC Proceedings Volumes*, 42(8):167–172, 2009. 7th IFAC Symposium on Fault Detection, Supervision and Safety of Technical Processes.

[16] P. Pillay R. Krishnan. Modeling, simulation, and analysis of permanent-magnet motor drives. the permanent-magnet synchronous motor drive. *IEEE Trans. on Industry Applications*, 25(2):265–273, 1989.

[17] M El Hachemi Benbouzid. A review of induction motors signature analysis as a medium for faults detection. *IEEE transactions on industrial electronics*, 47(5):984–993, 2000.

[18] D. HO and R.B. RANDALL. Optimisation of bearing diagnostic techniques using simulated and actual bearing fault signals. *Mechanical Systems and Signal Processing*, 14(5):763–788, 2000.

[19] Z. Zedong, L. Yongdong, M. Fadel, and X. Xi. A rotor speed and load torque observer for pmsm based on extended kalman filter. In *2006 IEEE International Conference on Industrial Technology*, pages 233–238, 2006.